Krylov Linear Solvers and Quasi Monte Carlo Methods for Transport Simulations

Sam Pasmann,[a] C. T. Kelley,[b] and Ryan McClarren*,[a]

[a] *Department of Aerospace and Mechanical Engineering*
University of Notre Dame
Fitzpatrick Hall, Notre Dame, IN 46556

[b] *North Carolina State University, Department of Mathematics*
3234 SAS Hall, Box 8205
Raleigh NC 27695-8205

*Email: rmcclarr@nd.edu

Number of pages:	17
Number of tables:	5
Number of figures:	6

Abstract

Keywords — Quasi Monte Carlo Methods, Krylov Linear Solvers

I. INTRODUCTION

Modeling the neutron transport equation (NTE) under various conditions, accurately, and efficiently is vital to nuclear reaction simulations like those in advanced reactor design or accident analysis [**?**]. The full form of the neutron transport equation describes the distribution of neutrons in space, angle, energy, and time. The high-dimensional nature of the problem has lead to many solution techniques most common of which have been stochastic Monte Carlo simulations or deterministic discrete ordinates (S_N) methods.

The standard diffusion accelerated Source Iteration (SI), is the simplest and common deterministic solution technique for solving the discrete ordinates method [**?**]. However, as the scattering and fission terms increase, the convergence rate of the Source Iteration can become arbitrarily small [**?**]. More advanced iteration techniques such as Krylov subspace methods, including Generalized Minimal RESidual method (GMRES) and BiConjugate Gradient STABilized method (BiCGSTAB), have been shown to outperform the standard Source Iteration, particularly when the scattering term is high [**?**, **?**]. Nonetheless, as the dimensionality of the problem increases, the quadrature techniques used to asses the system of equations becomes intractable [**?**].

Alternatively, Monte Carlo (MC) simulations provide a more robust solution, as the statistical error scales according to $O(N^{-0.5})$ regardless of the dimensionality of the problem CITATION. However, analog MC simulations are often seen as a *last resort* due to their high computational cost and slow rates of convergence [**?**]. Recent work by Willert et al. investigated a hybrid MC-deterministic solution in which the standard deterministic quadrature sweep of the iterative method is replaced with a Monte Carlo transport simulation [**?**, 2]. This technique attempts to combine the efficiency of iterative methods while also providing a tractable solution for complex problems given the robustness of MC simulation.

Although the MC simulation in this hybrid method benefits from a lower dimension problem, many particle histories are still required for convergence of the iterative method [2]. This work investigates the use of Quasi-Monte Carlo (QMC) techniques in place of standard MC to decrease the variance in the transport sweep and therefore increase the convergence rate of the iterative method. Quasi-Monte Carlo techniques use low-discrepancy sequences (LDS) in place of typical pseudo-random number generators for Monte Carlo sampling. Various LDS have been developed, including the Sobol and Halton sequences, where each attempts to sample the phase space in

a deterministic and uniform manner. Theoretically, this results in a sampling error of $O(N^{-1})$ as compared to $O(N^{-0.5})$ of standard Monte Carlo [**?**]. QMC is often used to evaluate complex integrals in fields like finance [**?**], but has largely been ignored by the particle transport community [**?**]. There has been some recent work in using QMC for radiation transport problems [**?**, **?**] but to the knowledge of the authors there has not been any recent work with QMC applied to neutron transport. This is likely because the deterministic nature of the LDS breaks the Markovian assumption needed for the particle random-walk. However, the iterative methods discussed allow the problem to be modeled as a pure absorber, where each particle is emitted and *traced* out of the volume without the need for a random-walk process.

To investigate this method, we focus on solving the one-dimensional, fixed-source neutron transport equation in slab geometry with isotropic sampling. This formulation is taken from [2] and can be seen in Equation 1. Although this is a reduced form of the full equation, it can still help evaluate the effectiveness of our methods.

$$\mu \frac{\partial \psi}{\partial x}(x,\mu) + \Sigma_t(x)\psi(x,\mu) = \frac{1}{2}\left[\Sigma_s(x)\int_{-1}^{1}\psi(x,\mu')\,d\mu' + q(x)\right] \text{ for } 0 \leq x \leq \tau \tag{1}$$

With boundary conditions:

$$\psi(0,\mu) = \psi_l(\mu), \mu > 0; \psi(\tau,\mu) = \psi_r(\mu), \mu < 0.$$

In the next section we present a brief overview of the Source Iteration, Krylov solvers, and proposed QMC methods. The results section contains analysis from three test problems. First, angular flux results from a problem that features a fixed boundary source in slab geometry with a spatially dependent exponentially decaying scattering cross section [1]. The second problem solves for scalar flux with multi-group data generated from FUDGE [**?**], in an infinite medium, and with a known analytic solution. The third and final problem known as *Reed's Problem*, provides an analytic solution for scalar flux across a mulit-media spatial domain [**?**] in slab geometry. Finally, key findings as well as future work is discussed in the conclusion.

II. METHODS

II.A. Source Iteration

Source iteration is Picard iteration for the fixed point problem. We begin with an initial guess ϕ_0 and solve Equation 1 for ψ_1. Given that:

$$\phi_n = \int_{-1}^{1} \psi_n d\mu. \tag{2}$$

That is, given ϕ_n compute ψ_{n+1}, then compute ϕ_{n+1} given Equation 2 until convergence where $\phi_{n+1} = \phi_n$. Given this iterative scheme, Equation 1 and Equation 2 combine to become:

$$\mu \frac{\partial \psi_{n+1}}{\partial x}(x,\mu) + \Sigma_t(x)\psi_{n+1}(x,\mu) = \frac{1}{2}\left[\Sigma_s(x)\phi_n(x) + q(x)\right]. \tag{3}$$

Given an angular discretization, this becomes a linear system of equations which, can be represented in operator notation where:

$$\phi = \mathcal{S}(\phi, q, \psi_l, \psi_r)$$

and

$$\mathcal{K}(\phi) = \mathcal{S}(\phi, 0, 0, 0) \text{ and } f = \mathcal{S}(0, q, \psi_l, \psi_r).$$

Where Source Iteration is represented as

$$\phi_{n+1} = \mathcal{K}(\phi_n) + f,$$

to get

$$A\phi \equiv (I - \mathcal{K})\phi = f$$

which we can send to a linear solver. It is important to note that the methods employed ensure that we never form the matrix A. Instead, the Monte Carlo simulation will compute the action of matrix A on ϕ.

II.B. Krylov Subspace Methods

An order-r Krylov subspace is defined with notation from the previous section as:

$$K_r = \text{span}(\phi, A\phi, A^2\phi, ..., A^{r-1}\phi). \tag{4}$$

For each experiment, two Krylov methods [6], GMRES [7] and Bi-CGSTAB [8], were used. The Generalized Minimum RESidual (GMRES) is one of the most common Krylov methods. When solving $A\vec{\phi} = \vec{f}$, GMRES minimized $||f - A\phi||_2$ over the k^{th} Krylov subspace. For every iteration, the GMRES stores an additional Krylov vector. For problems that require many iterations this may lead to memory constraints. Bi-CGSTAB is a low-storage Krylov method that is memory bounded throughout the algorithm. However, the memory savings come from information that is thrown out with each iteration and therefore Bi-CSTAB will generally require more iterations to converge than GMRES. Nonetheless, as we will in section IV, both Krylov methods will require far fewer iterations than the standard SI.

II.C. Monte Carlo Sweep

Monte Carlo methods for neutron transport seek to simulate the behavior of a statistically significant number of particles from *birth* to *death* to gain an approximate behavior of the system. For our 1-dimensional simulations, each particle begins with an initial position (x_i), direction (μ_i), and statistical weight (w_i). In an analog simulation, the particle would then be tracked from collision to collision, tallying quantities of interest in a defined spatial mesh. Each time the particle undergoes a collision, a new direction (μ) would be sampled and the next distance to collision would be calculated. This process would repeat until the particle is either absorbed or exits the volume. However, the invoked iterative methods allow the simulation to be modeled as a purely absorbing system. MC simulation in a purely absorbing system can be enhanced by employing the continuous weight absorption technique, which continuously reduces the statistical weight of each particle per length traveled (s):

$$w_1 = w_0 e^{-\Sigma_a s}. \tag{5}$$

Consequently, after emission the particle is traced straight out of the volume reducing the statistical weight according to the distance traveled across each spatial cell.

The track-length tally estimator is used to calculate the spatially-averaged scalar flux in the defined mesh. Because the weight is continuously reduced with each step, the tally scoring becomes:

$$\frac{1}{V}\int_0^s w_o e^{\Sigma_a s'} ds = \frac{1}{V}\left(\frac{1 - w_o e^{-\Sigma_a s}}{\Sigma_a}\right). \tag{6}$$

Neutron cross sections vary greatly with energy and contain large resonance regions, making them computationally expensive to model with high fidelity. The multigroup method is a common approach used to model energy-dependent cross sections in Monte Carlo. The multigroup method splits the energy range into G finite regions each with a representative cross section. In general geometry, the multigroup equations for G groups are:

$$\mu\frac{\partial\psi_g}{\partial x}(x,\mu) + \Sigma_{t,g}(x)\psi_g(x,\mu) = \frac{1}{2}\sum_{g'=1}^{G}\Sigma_{s,g'\to g}(x)\int_{-1}^{1}\psi_{g'}(x,\mu')\,d\mu' + \frac{q_g(x)}{2} \quad g = 1,\ldots,G. \tag{7}$$

The boundary conditions become:

$$\psi_g(0,\mu) = \psi_{l,g}(\mu), \mu > 0; \psi_g(\tau,\mu) = \psi_{r,g}(\mu), \mu < 0.$$

In matrix form, these equations are

$$\mu\frac{\partial\vec{\psi}}{\partial x}(x,\mu) + \underline{\Sigma}_t(x)\vec{\psi}(x,\mu) = \frac{1}{2}\underline{\Sigma}_s(x)\int_{-1}^{1}\vec{\psi}(x,\mu')\,d\mu' + \frac{\vec{q}(x)}{2}, \tag{8}$$

where

$$\vec{\psi} = (\psi_1,\psi_2,\ldots,\psi_G)^{\mathrm{T}}, \qquad \vec{q} = (q_1,q_2,\ldots,q_G)^{\mathrm{T}}, \tag{9}$$

$$\underline{\Sigma}_t(x) = \begin{pmatrix} \Sigma_{t,1}(x) & 0 & \ldots & \\ 0 & \Sigma_{t,2}(x) & 0\ldots & \\ \vdots & & \ddots & \\ 0 & \ldots & 0 & \Sigma_{t,G}(x) \end{pmatrix}, \tag{10}$$

and

$$\underline{\underline{\Sigma}}_s(x) = \begin{pmatrix} \Sigma_{s,1\to1}(x) & \Sigma_{s,2\to1}(x) & \dots & \Sigma_{s,G\to1}(x) \\ \Sigma_{s,2\to1}(x) & \Sigma_{s,2\to1}(x) & \dots & \Sigma_{s,G\to2}(x) \\ \vdots & \vdots & & \vdots \\ \Sigma_{s,G\to1}(x) & \Sigma_{s,G\to1}(x) & \dots & \Sigma_{s,G\to G}(x) \end{pmatrix}. \tag{11}$$

II.C.1. Quasi-Monte Carlo

Quais-Monte Carlo uses quasi-random low-discrepancy sequences in place of pseudo-random number generators in MC simulations. Low-discrepancy sequences use deterministic algorithms to sample the phase space in *self-avoiding* manner thereby approaching a more uniform distribution and approximating the expectation more efficiently. This results in a theoretical convergence rate of $O(N^{-1})$ compared to the $O(N^{-0.5})$ from pseudo-randomly placed points [**?**]. Because the low-discrepancy sequences sample the phases-space in a deterministic manner they introduce a dependence, albeit a weak one, on the dimensionality of the problem [**?**]. Commonly used low-discrepancy sequences include the Halton Sequence and Sobol Sequence [**?**]. For low-dimensional problems, the Halton sequence has been shown to provide the best results. However, for higher-dimensional problems the Sobol Sequence is most commonly used.

QMC is commonly used in Finance to evaluate high-dimensional integrals [**?**] and there has also been recent work in using QMC in radiative heat transfer applications [**?**, **?**]. However, QMC has largely been ignored by the particle transport community [**?**]. This is because the deterministic nature of the low discrepancy sequence breaks the Markovian assumption needed for the particle *random walk*. Therefore QMC must be implemented in specific applications which are not Markovian processes, such as the initial starting position of each particle, or steps must be take to ensure the Markovian assumption is held. Presently, there have been two separate strategies for implementing QMC in particle transport while maintaining the Markovian assumption. The first is known generally as randomized-QMC or (RQMC) which includes a host of strategies that attempt to reorder the sequence so each point is individually uniformly distributed within the space but the collective still retain their low-discrepency. [**?**, **?**, **?**, **?**, **?**]. The second, makes use of the previously discussed deterministic and iterative methods in which the problem can be modeled in the Monte Carlo simulation as a purely absorbing problem and the scattering term is iterated upon using one of the previously discussed methods removing the need for a *random walk* process

[?].

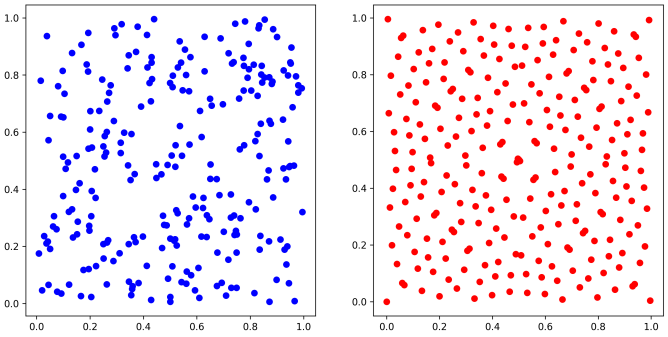

Fig. 1. 256 points generated in a unit square with pseudo random points (left) and the Sobol sequence (right).

III. IMPLEMENTATION

The program was written in Julia, a scientific computing language that combines the compiler capabilities of C++ and the syntax of Matlab and Python. The code and primary documentation are available here Krylov_QMC [?]. The linear and nonlinear solvers come from the Julia package SIAMFANLEQ.jl [3]. The documentation for these codes is in the Juila notebooks [4] and the book [5] that accompany the package.

IV. COMPUTATIONAL RESULTS

IV.A. Garcia-Siewert

The first computations use the problem from Garcia et al. [1], outlined in Table I, and consider two cases for the scattering cross section ($\Sigma_s = e^{-x/s}$), $s = 1$ and $s = \infty$. First, we solve the QMC linear problem with $N = 2048$ and $N_x = 100$. Figure 2 shows that for an exponentially decaying scattering cross section ($s = 1$) the Krylov iterations take fewer than a third of the number of transport sweeps than that of the Picard iteration for a relative residual of 10^{-9}. While Figure 3 ($s = \infty$) shows the Krylov iterations took less than 25 iterations to reach a relative error of 10^{-6} while the Picard iteration required nearly 200 iterations.

TABLE I
Parameters for fixed boundary source, slab geometry, simulation from Garcia et al. [1]

Parameter	Value
Σ_t	1
$\Sigma_s(x)$	$e^{-x/s}$
τ	5
$\psi_l(\mu)$	1
$\psi_r(\mu)$	0
N_x	50
$q(x)$	0

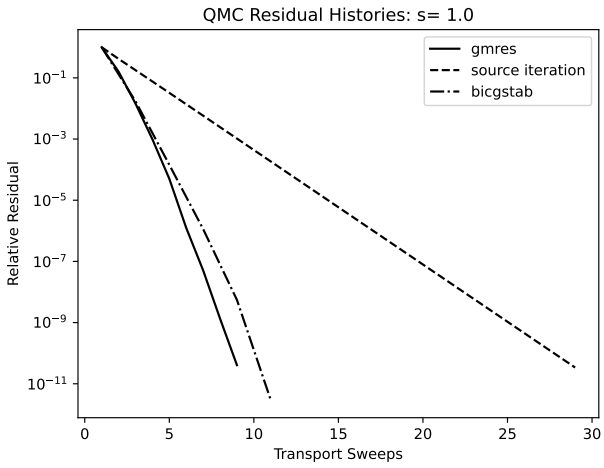

Fig. 2. Scalar flux relative residuals for $s = 1$ given parameters from Table I and $N = 2048$.

IV.A.1. Validation and calibration study

We conclude this problem with a validation study. We compare the QMC results with the results from [1]. The results in [1] are exit distributions and are accurate to six figures. We have duplicated those results with an S_N computation on a fine angular and spatial mesh.

For $N = 2048$ and $Nx = 100$ we obtain the cell-average fluxes from the QMC approximation. We then use a single S_N transport sweep to recover the exit distributions from the QMC cell-average fluxes. We report the results and the corresponding results from [1] in Tables II and III. The exit distributions, as is clear from Table II can vary by five orders of magnitude. Even so, the results from QMC agree with the benchmarks to roughly two figures.

In Tables IV and V we look at the relative errors in the QMC exit distributions as compared to a highly accurate S_N result. We compensate for the widely varying scales by tabulating, for

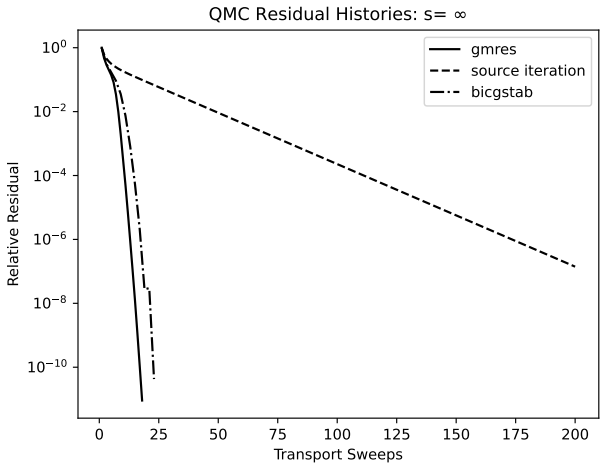

Fig. 3. Scalar flux relative residuals for $s = \infty$ given parameters from Table I and $N = 2048$.

each value of N and Nx

$$R = \max(R^0, R^\tau)$$

where

$$R^0 = \max_\mu \frac{|\psi^{SN}(0,-\mu) - \psi^{QMC}(0,-\mu)|}{\psi^{SN}(0,-\mu)}$$

and

$$R^\tau = \max_\mu \frac{|\psi^{SN}(\tau,\mu) - \psi^{QMC}(\tau,\mu)|}{\psi^{SN}(\tau,\mu)}.$$

IV.B. Multigroup Problems

The second problem features 12, 70, and 618 group cross section data of high-density polyethylene generated with FUDGE [**?**] in an infinite medium. The analytic solution of the scalar flux is given by:

$$\phi = (\Sigma_t - \Sigma_s)^{-1} Q. \tag{12}$$

These are preliminary results with $N_x = 40$ and $N = 2^{10}$. We may want to make these larger and/or make tables like Table IV and Table IV.

IV.C. Reed's Problem

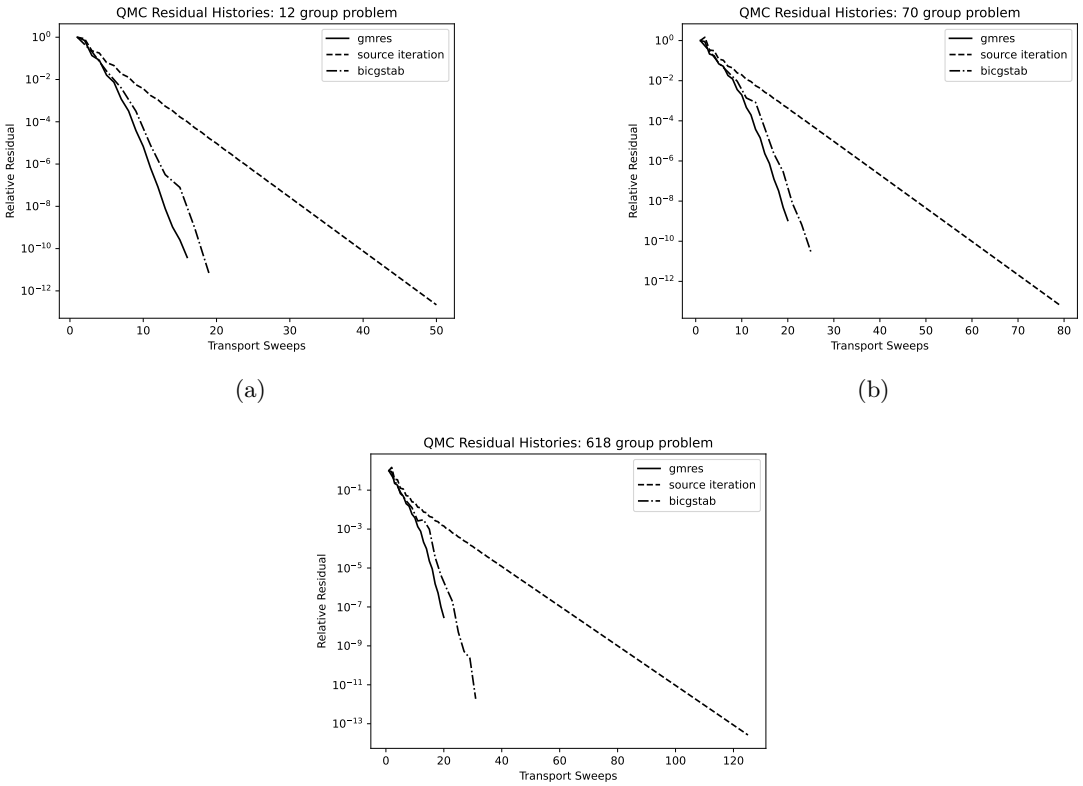

(a) (b)

(c)

Fig. 4. Multigroup relative residuals

TABLE II
Angular flux exit Distributions from Garcia/Siewart and the S_N QMC sweep (with $N = 2048$ and $Nx = 100$), along with difference between results for $s = 1$.

	Garcia/Siewert		QMC		Difference	
μ	$\psi(0,-\mu)$	$\psi(\tau,\mu)$	$\psi(0,-\mu)$	$\psi(\tau,\mu)$	$\psi(0,-\mu)$	$\psi(\tau,\mu)$
0.05	5.89664e-01	6.07488e-06	6.07035e-01	5.91908e-06	test	test
0.10	5.31120e-01	6.92516e-06	5.47466e-01	6.74075e-06	test	test
0.20	4.43280e-01	9.64232e-06	4.57064e-01	9.35453e-06	test	test
0.30	3.80306e-01	1.62339e-05	3.92223e-01	1.56108e-05	test	test
0.40	3.32964e-01	4.38580e-05	3.43481e-01	4.13721e-05	test	test
0.50	2.96090e-01	1.69372e-04	3.05510e-01	1.58622e-04	test	test
0.60	2.66563e-01	5.73465e-04	2.75098e-01	5.39514e-04	test	test
0.70	2.42390e-01	1.51282e-03	2.50192e-01	1.43257e-03	test	test
0.80	2.22235e-01	3.24369e-03	2.29422e-01	3.08975e-03	test	test
0.90	2.05174e-01	5.96036e-03	2.11837e-01	5.70555e-03	test	test
1.00	1.90546e-01	9.77123e-03	1.96756e-01	9.39189e-03	test	test

TABLE III
Angular flux exit Distributions for: $N = 2048$, $Nx = 100$, and $s = \infty$.

	Garcia/Siewert		QMC	
μ	$\psi(0,-\mu)$	$\psi(\tau,\mu)$	$\psi(0,-\mu)$	$\psi(\tau,\mu)$
0.05	8.97798e-01	1.02202e-01	9.06050e-01	1.03680e-01
0.10	8.87836e-01	1.12164e-01	8.95849e-01	1.13695e-01
0.20	8.69581e-01	1.30419e-01	8.76487e-01	1.31907e-01
0.30	8.52299e-01	1.47701e-01	8.58937e-01	1.49245e-01
0.40	8.35503e-01	1.64497e-01	8.42195e-01	1.66128e-01
0.50	8.18996e-01	1.81004e-01	8.25870e-01	1.82734e-01
0.60	8.02676e-01	1.97324e-01	8.09780e-01	1.99151e-01
0.70	7.86493e-01	2.13507e-01	7.93834e-01	2.15421e-01
0.80	7.70429e-01	2.29571e-01	7.77997e-01	2.31558e-01
0.90	7.54496e-01	2.45504e-01	7.62269e-01	2.47547e-01
1.00	7.38721e-01	2.61279e-01	7.46673e-01	2.63362e-01

TABLE IV
Exit Distributions Errors: $s = 1.0$

Nx \N	1024	2048	4096	8192	16384
50	1.31716e-01	1.34260e-01	1.35123e-01	1.35328e-01	1.35242e-01
100	6.09631e-02	6.35764e-02	6.46191e-02	6.48898e-02	6.48536e-02
200	3.77223e-02	3.12496e-02	3.12005e-02	3.17337e-02	3.16710e-02
400	2.63214e-02	1.45106e-02	1.52355e-02	1.56636e-02	1.56854e-02
800	2.39486e-02	9.94925e-03	7.24627e-03	8.86212e-03	7.84063e-03
1600	4.16277e-02	9.95048e-03	5.11618e-03	8.02709e-03	4.44021e-03
3200	4.60905e-02	1.07345e-02	4.45922e-03	7.49522e-03	3.76179e-03

TABLE V
Exit Distributions Errors: $s = \infty$

Nx \N	1024	2048	4096	8192	16384
50	1.31716e-01	1.34260e-01	1.35123e-01	1.35328e-01	1.35242e-01
100	6.09631e-02	6.35764e-02	6.46191e-02	6.48898e-02	6.48536e-02
200	3.77223e-02	3.12496e-02	3.12005e-02	3.17337e-02	3.16710e-02
400	2.63214e-02	1.45106e-02	1.52355e-02	1.56636e-02	1.56854e-02
800	2.39486e-02	9.94925e-03	7.24627e-03	8.86212e-03	7.84063e-03
1600	4.16277e-02	9.95048e-03	5.11618e-03	8.02709e-03	4.44021e-03
3200	4.60905e-02	1.07345e-02	4.45922e-03	7.49522e-03	3.76179e-03

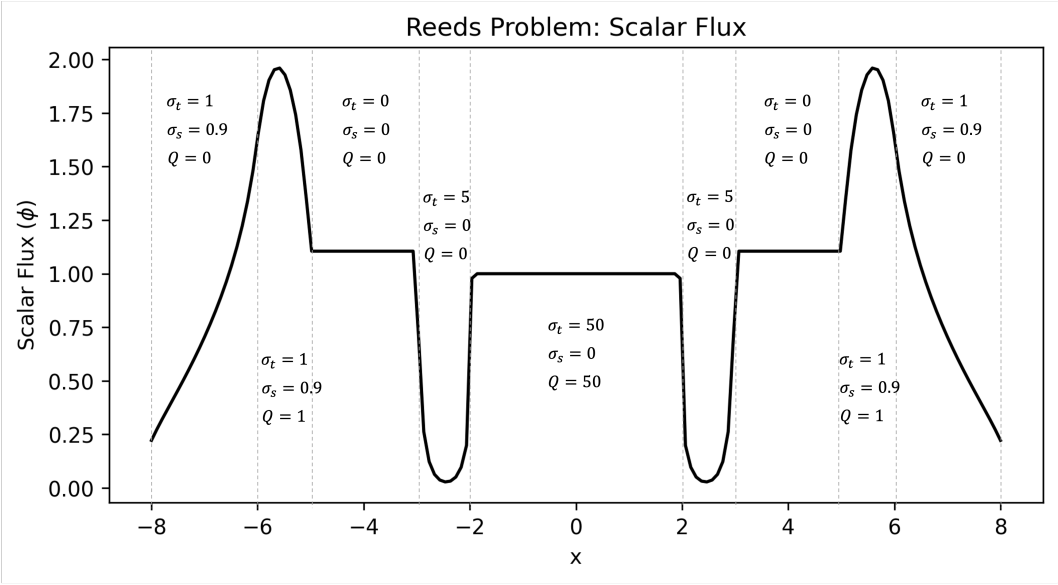

Fig. 5

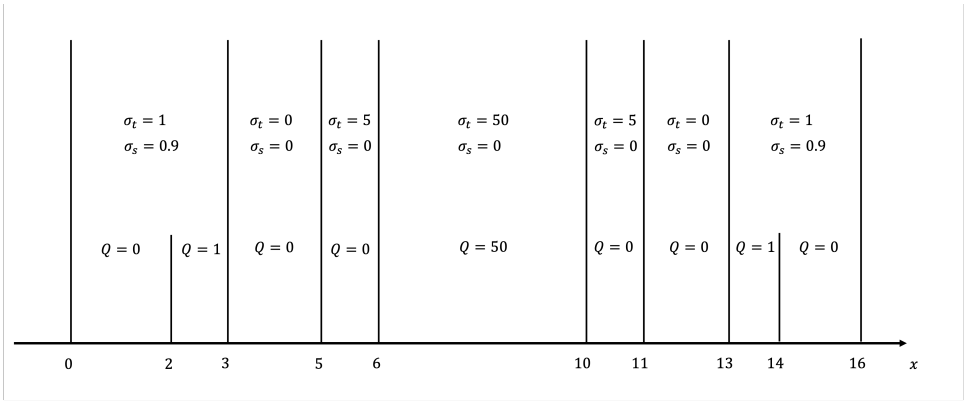

Fig. 6

V. CONCLUSION

ACKNOWLEDGMENTS

This work was funded by the Center for Exascale Monte-Carlo Neutron Transport (CEMeNT) a PSAAP-III project funded by the Department of Energy, DE-NA003967, and supported by National Science Foundation Grants DMS-1745654, and DMS-1906446.

REFERENCES

[1] R. Garcia and C. Siewert, "Radiative transfer in finite inhomogeneous plane-parallel atmospheres," *J. Quant. Spectrosc. Radiat. Transfer*, **27**, 141 (1982).

[2] J. Willert, C. T. Kelley, D. A. Knoll, and H. K. Park, "Hybrid Deterministic/Monte Carlo Neutronics," *SIAM J. Sci. Comp.*, **35**, S62 (2013).

[3] C. T. Kelley, "SIAMFANLEquations.jl," https://github.com/ctkelley/SIAMFANLEquations.jl (2020); 10.5281/zenodo.4284807., URL https://github.com/ctkelley/SIAMFANLEquations.jl, julia Package.

[4] C. T. Kelley, "Notebook for Solving Nonlinear Equations with Iterative Methods: Solvers and Examples in Julia," https://github.com/ctkelley/NotebookSIAMFANL (2020); 10.5281/zenodo.4284687., URL https://github.com/ctkelley/NotebookSIAMFANL, iJulia Notebook.

[5] C. T. Kelley, "Solving Nonlinear Equations with Iterative Methods: Solvers and Examples in Julia," (2020)Unpublished book ms, under contract with SIAM.

[6] C. T. Kelley, *Iterative Methods for Linear and Nonlinear Equations*, no. 16 in Frontiers in Applied Mathematics, SIAM, Philadelphia (1995).

[7] Y. Saad and M. Schultz, "GMRES a generalized minimal residual algorithm for solving nonsymmetric linear systems," *SIAM J. Sci. Stat. Comp.*, **7**, 856 (1986).

[8] H. A. van der Vorst, "Bi-CGSTAB: A fast and smoothly converging variant to Bi-CG for the solution of nonsymmetric systems," *SIAM J. Sci. Statist. Comput.*, **13**, 631 (1992).